# A Modelling Study of Seasonal Borehole Thermal Energy Storage in Scotland: Integrating Surface Demand and the Subsurface Heat Store

Proceedings World Geothermal Congress 2023
Beijing, China, April 17 – 21, 2023

# A Modelling Study of Seasonal Borehole Thermal Energy Storage in Scotland: Integrating Surface Demand and the Subsurface Heat Store

Isa Kolo[1], Christopher S Brown[1], Andrew Lyden[2], Sean Watson[1,3], David Banks[1], Gioia Falcone[1], Daniel Friedrich[2]

[1]James Watt School of Engineering, University of Glasgow, Glasgow, G12 8QQ, UK. [2]School of Engineering, Institute for Energy Systems, University of Edinburgh, Colin Maclaurin Road, Edinburgh, EH9 3DW, UK. [3]TownRock Energy, East Woodlands House, Dyce, Aberdeen, AB21 0HD

Isa.Kolo@glasgow.ac.uk, Christopher.Brown@glasgow.ac.uk, Andrew.Lyden@ed.ac.uk, Sean.Watson@townrock.com, Gioia.Falcone@glasgow.ac.uk, David.Banks@glasgow.ac.uk, D.Friedrich@ed.ac.uk

**Keywords:** Borehole Thermal Energy Storage, Borehole Heat Exchanger, Solar Thermal, Building Heat Demand, Seasonal Thermal Energy Storage, University of Glasgow, James Watt Building, OpenGeoSys, Atlite

## ABSTRACT

In the UK, 80% of heat is currently supplied by combustion of natural gas, which significantly contributes to the country's greenhouse gas emissions. This makes it imperative to explore alternative energy sources in the drive towards a net-carbon-zero economy. Geothermal energy is a renewable energy source that can provide reliable low-carbon energy baseload for direct heat use. In addition to the UK's large demand for direct heat use in the winter, significant cooling demand exists in the summer. Hence, seasonal underground thermal energy storage should be considered. Borehole thermal energy storage (BTES), in which the subsurface serves as the storage medium via borehole heat exchanger (BHE) arrays, is particularly attractive since it can technically be applied anywhere provided there is little significant groundwater flow.

In this work, the James Watt building at the University of Glasgow is taken as the basis for a modelling study. A low-temperature BTES system is employed to meet the building's seasonal heating/cooling demands by numerical modelling on OpenGeoSys software coupled to TESPy, incorporating the subsurface BHE and a heat pump. BTES is chosen due to the absence of a suitable shallow aquifer for aquifer thermal energy storage and lack of surface footprint for pit or tank thermal energy storage. The change in BHE fluid inlet and outlet temperatures as well as ground temperature throughout one year of operation have been studied. Results indicate that thermal energy can be stored during summer and extracted during winter. A solar-thermal system is used to meet the demand of the James Watt building in the summer (1030 MWh) while a surplus of 318 MWh is stored for use in the winter. The stored heat is extracted in the winter, and it contributes to 16% of the building's winter demand (i.e., 318 MWh of a total winter demand of 1981 MWh).

## 1. INTRODUCTION

Heating and cooling account for about half of the energy consumption in the EU and UK (EC, 2020; BEIS, 2021). In the UK, 37% of carbon emissions come from heating and only 7.3% of the heating and cooling demand is met using renewable energy sources (Energy Systems Catapult, 2022; BEIS, 2022). With the UK Government's target of reaching net zero carbon emissions by 2050, heating and cooling must be further decarbonised (BEIS, 2020). This can be achieved by exploring renewable energy sources such as solar energy. Solar energy can be used for heating through solar-thermal collectors and via electricity generation through photovoltaic panels. Solar energy is a seasonal resource, with its availability biased towards summer. Through solar-thermal collectors, solar energy can be converted to heat, however, heat demand is higher in the winter. Additionally, waste heat from air conditioning and space cooling is often available during summer. Thus, solar, and surplus building-thermal energy needs to be stored in the summer to be used in the winter when there is high heat demand, i.e., seasonal thermal energy storage (STES).

There are various forms of STES including (i) above-surface storage with tank thermal energy storage and pit thermal energy storage, and (ii) underground thermal energy storage (UTES) through boreholes, networks of heat exchange pipes, aquifers, or flooded mines. The focus of this work is UTES where there is little available land footprint on the surface. Of the UTES types, borehole thermal energy storage (BTES) has wider applicability and fewer geological limitations (Lyden *et al*., 2022). No special aquifer or mine workings are needed; the main requirement is limited groundwater flow (which can advect heat away from the store). Due to the relatively small temperature difference between the ground and heat transfer fluid, a heat pump is often used together with the BTES system to raise the fluid temperature for end use (Gao *et al*., 2015) although there are examples of high-temperature storage, where heat pumps are not required (e.g., Drake Landing (Sibbitt et al., 2012)). There are many systems in the world using BTES for storage of solar-thermal heat (we refer to this as solar borehole thermal energy storage – SBTES) such as in Germany, Canada, Italy, and Netherlands (Xu *et al*., 2014; Gao *et al*., 2015). Figure 1 shows the operation of an SBTES system in summer and winter. Heat is exchanged with the ground through a borehole heat exchanger (BHE) which is a tube with a heat transfer fluid. In the summer, heat harvested from the solar collectors is transferred to the ground through the heat transfer fluid in the BHE. In the winter, the heat stored in the ground is extracted and fed into a building for end-use, for example, in space heating. Typically, a heat pump is used when extracting heat from the BHE before reaching the end-user. There are different types of BHE shapes that can be used – a single U-tube, a double U-tube, or a coaxial (concentric) tube. The use of a coaxial BHE for extraction is highlighted in figure 1, where the cold fluid enters through the annulus and exits, after gaining heat, through the central outlet.

There is significant research interest in SBTES systems due to their potential to decarbonise heating (Yuan *et al.*, 2022). Wang and Qi (2008) analysed the performance of an SBTES system including a water storage tank for a residential building in China using experiments and numerical simulations. Their work showed that the intensity of the solar radiation and proper size-match between

the storage water tank and the area of solar collectors, significantly affect the performance of the BTES system; a storage efficiency of up to 40% was recorded for the BTES system (although thermal storage efficiency is an elusive concept, see Skarphagen et al. (2019) and Brown et al. (2022)). While construction of an actual pilot system is ideal to demonstrate BTES, it can be expensive, time-consuming, and restrictive to investigate a wide range of operational scenarios/periods using experiments. Thus, as adopted by Wang and Qi (2008), numerical modelling is a more flexible and common approach for analysing SBTES systems.

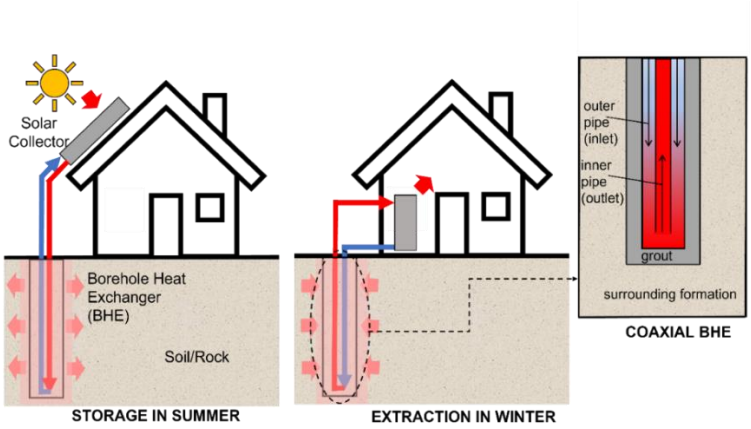


**Figure 1: Schematic of the simplified operation of a Solar Borehole Thermal Energy Storage (SBTES) System. A single borehole is shown for simplicity. However, single boreholes are not efficient at heat storage and a compact array of numerous shallow boreholes is typically required for storage efficiency.**

TRNSYS is a semi-analytical tool which is commonly used to model whole thermal systems including surface and subsurface components (Andrew *et al.*, 2022). Using TRNSYS, Pahud (2000) studied optimal operation conditions of an SBTES system in a typical Swiss setting. For a ground with thermal resistance of 2.5 W/m/K, an optimal spacing of 2.5 m between boreholes was determined. Nordell and Hellström (2000) conducted another study of a residential area at Danderyd, Sweden, using TRNSYS and MINSUN with the latter simulating the thermal behaviour of the solar heating system. This SBTES system was for an annual heat demand of 1080 MWh, utilising 3000 $m^2$ of solar collectors with a solar fraction of 60%. They proposed a 60,000 $m^3$ array storage with 99 boreholes of 65 m depth and 3 m spacing. Storage temperatures varied between 30°C and 45°C over the year. They also noted that increasing the size of the BTES arrays would reduce heat losses from the system thereby improving the overall system efficiency. The performance of the Drake Landing (Canada) Solar Community project was analysed over an operational 5-year period and results showed that initial performance predictions using TRNSYS were accurate (Sibbitt et al., 2012). More recently, Yuan *et al.* (2022) used TRNSYS to investigate an SBTES system for district heating of a residential area in Espoo, Finland. They proposed a hybrid district heating system with solar energy which uses BTES to meet part of the heat demand in the winter. The heat pump was operated by electricity generated from photovoltaic panels. Their results showed that 38 – 58% of total heat demand can be met using heat energy harvested on-site translating to 31 – 66% reduction in carbon emissions compared to the non-hybrid system. Kubinski *et al.* (2020) used Aspen HYSYS and Salvestroni *et al.* (2021) used TRNSYS for solar-thermal energy storage in Danish and Italian contexts, respectively, where tank thermal energy storage was adopted for seasonal storage. Schach *et al.* (2018) established that gas-heating systems have similar costs in comparison to decentralised heat supply systems with BTES. The control strategy of the SBTES system is also very important and can lead to reductions in cost and carbon emissions (Saloux *et al.*, 2021). Moreover, investigations by Maximov *et al.* (2021) revealed that, compared to a gas-heating system, the use of BTES can improve system performance and reduce carbon emissions by up to 90% while increasing the levelised cost of energy by less than 20%. These studies suggest that the use of BTES can significantly contribute to the net zero targets of the UK Government.

In this work, a notional case study of SBTES is considered where solar-thermal collectors are installed on the James Watt Building of the University of Glasgow and a BTES system is used for seasonal thermal energy storage. The simulation of available solar energy is performed using the open-source Python package Atlite while the BTES system is simulated using the open-source finite element software, OpenGeoSys, with geological parameters representative of the area close to the University of Glasgow. For the surface components, including header-pipe manifolds and heat pump, TESPy is coupled to OpenGeoSys. The BTES system is sized based on the heat demand of the building and a full year of system operation is simulated. Focus is on underground thermal energy storage to investigate the fluid and rock temperatures. The aim of the study is to establish the BTES array size and operating conditions that would make it feasible to meet the building heat demand.

## 2. GEOLOGICAL SETTING

The geology around the University of Glasgow is inferred from boreholes drilled close to the university. The campus is underlain by Devensian glacial deposits of till, clay, and silt, and bedrock of the Namurian age Limestone Coal Formation, part of the Carboniferous Clackmannan Group. The Carboniferous stratigraphy beneath western Glasgow is dominated by cyclic successions of sedimentary rocks of the Strathclyde and Clackmannan Groups. These strata consist of sandstones and mudstones, with limestones, coals, ironstones and seatearths, laid down in fluvial and fluviodeltaic environments established following the submergence of Lower Carboniferous volcanic terrains (Forsyth *et al.*, 1996; Hall *et al.*, 1998). Data from four boreholes have been used to establish the stratigraphy around the university: University of Glasgow University No. 7 borehole (NS 57016 66584; BGS borehole reference NS56NE458), Queenslie No. 2 borehole (NS 65895 64900; BGS NS66SE49), South Balgray or Gartnavel No. 3 borehole (NS 55780 67810; BGS NS56NE369; Watson et al. 2019) and Hurlet borehole (NS 51110 61230; BGS NS56SW333) (Watson, 2022). For the purposes of this simulation, we have assumed a single lithology, the Limestone Coal Formation, with isotropic and homogeneous thermal properties based on harmonic mean values calculated by Watson (2021) as follows: thermal

conductivity $\lambda_s$ 1.82 W/(m·K), bulk density $\rho_s$ 2558 kg/m$^3$, specific heat capacity $c_{ps}$ 806 J/(kg·K), implying a bulk volumetric heat capacity of 2.06 MJ/(m$^3$·K).

The ground surface air temperature assumed for the present study is 10.17 °C. This is the mean annual surface air temperature for 2021, calculated from measured data from the Paisley Coats Meteorological Office Observatory (Met Office, 2022). The most reliable subsurface temperature measurements made within the vicinity of the University of Glasgow, were made in the Maryhill borehole (NS 57178 68558; BGS NS56NE1755). A total of 99 temperature measurements were made in the borehole to a depth of 303 m, as well as 82 thermal conductivity measurements on borehole core (Browne et al., 1987). A geothermal gradient of 35.92 °C/km was calculated based upon the measured temperature dataset.

## 3. METHODS

A schematic of the complete SBTES system is shown in figure 2. In the summer, the heat from the solar collectors is used to meet the demand of the building and excess heat is stored, initially in a buffer tank of nominal 18 days' buffer storage capacity, to smooth out peaks in heat supply and demand, and then long-term surplus heat is directed to a BTES store. During winter, stored heat is released gradually from the BTES to supplement heat supply to the building (most likely via a heat pump, which is not explicitly modelled here).

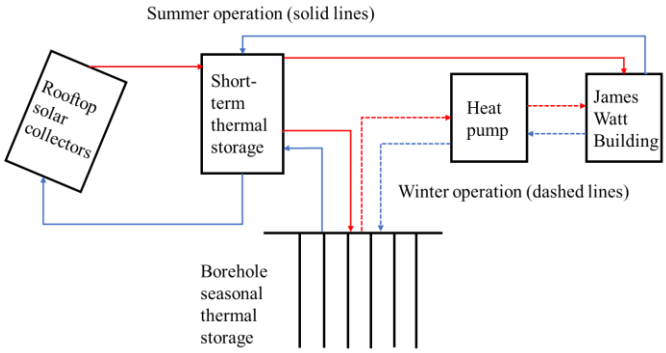


Figure 2: A schematic of the solar borehole thermal energy storage for the James Watt building.

### 3.1 Borehole Heat Exchanger (BHE) and Heat Pump Modelling

The finite element code OpenGeoSys is used to model the BHE. OpenGeoSys implements an optimal discretisation approach which does not fully discretise the BHE and the surrounding rock formation potentially leading to a prohibitively large finite element mesh. Rather, the 'dual-continuum' approach (Al-Khoury *et al.*, 2010; Diersch *et al.*, 2011) is adopted which discretises the BHE using one-dimensional elements while the surrounding rock formation is fully discretised using three-dimensional prism elements (Chen *et al*., 2019). The governing equations for heat transfer are solved in three computational domains which are linked by boundary conditions: (1) the inflow and outflow pipes of the BHE which are convection-dominated; (2) the grout in which conduction is dominant; and (3) the surrounding rock formation which is also dominated by conduction (groundwater flow being assumed to be absent). The grout is a cementitious material placed between the borehole casing and the formation to stabilise the borehole and prevent uncontrolled fluid flow along the annulus between borehole wall and casing, see figure 1.

OpenGeoSys can handle different BHE tube shapes including single U, double U, and different flow configurations of the coaxial pipe. Although shallow BHEs predominantly use the U-tube configuration, we have chosen, in this study, to simulate coaxial BHE, as they can have lower borehole thermal resistance than U-tube configurations (Quaggiotto *et al.*, 2019). We have chosen to simulate coaxial closed loop boreholes, although Andersson et al. (2021) suggest that practical issues with their installation and operation at Emmaboda, Sweden might lead them to favour U-tubes (despite their theoretically somewhat less favorable thermal efficiency) in future projects. Details of governing equations and boundary conditions can be found in Chen *et al.* (2019) and Kolo *et al.* (2022). OpenGeoSys has been verified against analytical solutions and other numerical solutions (Chen *et al.*, 2019; Kolo *et al.*, 2022). The coaxial pipe configuration has also been validated using real data (Cai *et al*, 2021).

To combine the BHEs together in a pipe network, OpenGeoSys can be coupled to TESPy which is an opensource software that simulates powerplants. Through this coupling, surface components such as heat pumps can be added to the network (Cai *et al*, 2021). The heat transfer fluid is distributed to the BTES via a common hydraulically balanced manifold ("splitter") which distributes it evenly to all BHEs at the same inlet temperature. The return fluid flows from the individual BHEs (which will have subtly different temperatures) are combined in another manifold (the "merger") before entering the heat pump. The heat pump is assumed, but not explicitly modelled in this paper: i.e., we discuss only the heat extracted from the BTES, not the heat eventually delivered to the building.

### 3.2 Solar Modelling

Solar thermal collectors convert solar energy into heat which can be used for space and water heating as well as district heating. The open-source Python package Atlite (Hofmann *et al*., 2020) was used to model the energy output of roof-mounted solar thermal collectors for the James Watt building on the University of Glasgow campus. The area covered by the building is highlighted in figure 3.


**Figure 3: Left: Map of the UK highlighting the location of the James Watt building of the University of Glasgow; Right: Total area of the James Watt building: 3193.53 m$^2$ (Google Maps, 2022).**

Hourly heat output from solar collectors was calculated using actual hourly average global radiation on the solar collector and the difference between the connected thermal storage temperature and the hourly average ambient air temperature, see Henning and Plazer (2014) for full methodology. The global radiation was sourced from the ERA5 reanalysis weather dataset (Hersbach *et al.*, 2020). Table 1 contains the set of assumptions for the solar collector technology.

**Table 1: Assumptions for solar collector technology. Note that $C_0$ and $C_1$ are efficiency coefficients.**

| Parameter | Value |
|---|---|
| Azimuth | 180° |
| Slope | 40° |
| $C_0$ | 0.8 |
| $C_1$ | 3.0 |
| Temperature of connected store | 80°C |

For the James Watt building, Google Map images were used to measure the total roof space (3193.53m$^2$). Hourly heat generation profiles were produced assuming that, in addition to the full roof size, there are additional solar panels having a total area of half the roof size, i.e., total area of solar panels is 1.5 times the roof size of the James Watt building. This extra space can be provided by the neighbouring Thomson building (see figure 3).

### 3.3 Source of Charge: Heat Demand and Surplus Solar Heat

The 2021 building heat demand for the James Watt building is used in this study; the building has an annual heat demand of 3011 MWh of which 1981 MWh is in the winter (defined as months October to March). Heat from the solar collectors is first used to meet the building demand, via a surface buffer tank of c. 18 days' thermal capacity, allowing *surplus* heat to be stored. This allows peaks in solar heat supply to be smoothed before the 18-day surplus is directed to the BTES for long-term storage. The effect of the tank has simply been simulated by applying an 18-day moving average to the surplus solar energy supply. Figure 4 shows the building heat demand, heat available from the solar collectors and the surplus heat. Figure 5 shows the heat supplied to the BTES, resulting from the 18-day moving average: a peak charge of 7.7 MWh/day (322 kW – consistent with table 2) and an 18-day cumulative peak charge of 139 MWh or 500.4 GJ.

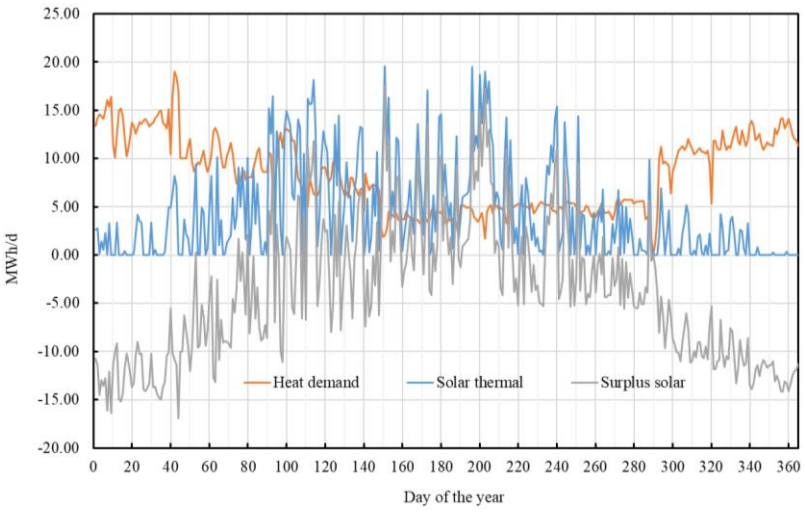


**Figure 4: Annual demand of James Watt building, heat from solar-thermal and surplus solar heat after meeting building heat demand.**

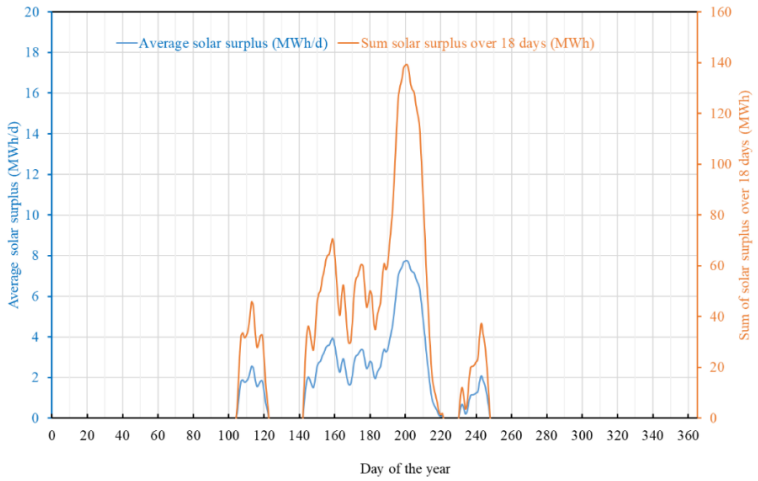


**Figure 5: 18-day moving average showing average solar surplus and sum of solar surplus over 18 days.**

Based on Figure 5 (for 2021 only), we have used the following charge profile for surplus solar heat from the intermediate store to the BTES, resulting in a total of 318 MWh being delivered to the BTES between April and September (Table 2), at a peak charge rate of 322 kW. We have assumed that the BTES is evenly discharged between November and February at a rate of 79.5 MWh per month, at a peak discharge rate of 200 kW.

**Table 2: The plan for simulated BTES storage and extraction: Charging regime (summer) for the storage of 317.92 MWh and discharging regime (winter) for the extraction of the stored heat.**

| Month | Heat charged to BTES (MWh) | Average monthly rate (kW) | Peak charge rate (kW) | Duration of peak charge (days) |
|---|---|---|---|---|
| J | | | | |
| F | | | | |
| M | | | | |
| A | 28.04 | 38.9 | 106 | 2 |
| M | 17.95 | 24.1 | 113 | 2 |
| J | 86.50 | 120.1 | 163 | 2 |
| J | 160.56 | 215.8 | 322 | 4 |
| A | 19.68 | 26.3 | 98 | 2 |
| S | 5.28 | 7.3 | 77 | 2 |
| O | | | | |
| N | | | | |
| D | | | | |
| Total | 317.92 | | | |

**Charging Regime**

| Month | Heat extracted from BTES (MWh) | Average monthly rate (kW) | Peak extraction rate (kW) | Duration of peak extraction (hours) |
|---|---|---|---|---|
| J | 79.48 | 106.8 | 200 | 12 |
| F | 79.48 | 118.3 | 200 | 12 |
| M | | | | |
| A | | | | |
| M | | | | |
| J | | | | |
| J | | | | |
| A | | | | |
| S | | | | |
| O | | | | |
| N | 79.48 | 110.4 | 200 | 12 |
| D | 79.48 | 106.8 | 200 | 12 |
| Total | 317.92 | | | |

**Discharging Regime**

### 3.4 BHE Array Sizing

The capacity of the BTES is 318 MWh or 1144.8 GJ which is the total amount of heat to be stored and discharged over an annual cycle. The volume of ground required for a BTES can be estimated by equation (1)

$$V_{\max} = \frac{H_{\max}}{(\rho c)_m \Delta T} \tag{1}$$

in which $H_{\max}$ is the maximum heat load of 1144.8 GJ, $(\rho c)_m$ is the volumetric heat capacity of the rock (assumed 2.2 MJ/m$^3$/K) and $\Delta T$ is average the temperature rise (assumed 15K). This results in a volume of 34690 m$^3$ required for storage. Assuming an equidimensional cylinder (diameter=height), the height of the cylinder, $h = 2r$ where $r$ is the radius. Thus, the volume of the equidimensional cylinder is given by:

$$V_{cyl} = \pi r^2 h = 2\pi r^3 \tag{2}$$

For the volume, $V_{cyl}$ = 34690 m$^3$, radius of the BHE array volume is $r \approx 18$ m. Hence, the storage volume is a cylinder with an 18 m radius and 36 m deep. The surface area of the array is $\pi r^2$ = 1018 m$^2$.

The number of boreholes required is found based on the maximum heat exchange rate – 322 kW. Assuming a specific heat extraction rate of 40 W/m implies that 8050 m of borehole is required. This translates to 224 boreholes that are 36 m deep. For a surface area of 1018 m$^2$, there should be one borehole for every 4.54 m$^2$. When a square packing of boreholes is assumed, the spacing is $\approx$ 2.13 m.

### 3.5 Parameterisation

The assumptions made for the BTES system are listed in table 3 (Schulte et al., 2016) including some geological parameters (Watson, 2022). In this preliminary study, an anti-freeze is used as the heat transfer fluid – monoethylene glycol at 23.5 wt%. At 10°C, it has a density of 1032 kg/m$^3$, specific heat capacity of 3842 J/kg/K, and thermal conductivity of 0.482 W/m/K (Melinder, 2010). No insulation is assumed on the ground at the surface.

**Table 3. Parameters of BTES system**

| Parameter | Value | Units | Symbol |
|---|---|---|---|
| Diameter of Borehole | 0.152 | m | |
| Inner Diameter of Outer Pipe | 0.127 | m | |
| Inner Diameter of Inner Pipe | 0.087 | m | |
| Thickness of Inner Pipe | 0.0055 | m | |
| Thickness of Outer Pipe | 0.0056 | m | |
| Thermal Conductivity of Inner Pipe | 0.42 | W/(m·K) | |
| Thermal Conductivity of Outer Pipe | 0.42 | W/(m·K) | |
| Density of Grout | 2190 | kg/m$^3$ | $\rho_g$ |
| Thermal Conductivity of Grout | 1.5 | W/(m·K) | $\lambda_s$ |
| Specific Heat Capacity of Grout | 1735 | J/(kg·K) | $c_{pg}$ |
| Density of Fluid | 1032 | kg/m$^3$ | $\rho_f$ |
| Thermal Conductivity of Fluid | 0.482 | W/(m·K) | $\lambda_f$ |
| Specific Heat Capacity of Fluid | 3842 | J/(kg·K) | $c_{pf}$ |
| Initial inlet Temperature of Fluid | 10 | °C | |
| Surface Temperature | 10.17 | °C | |
| Geothermal Gradient | 35.92 | °C/km | |
| Volumetric Flow Rate per Borehole | 0.000112 | m$^3$/s | |
| Total Volumetric Flow Rate for BTES | 0.025 | m$^3$/s | |

### 3.6 Subsurface Model Set-up and Boundary Conditions

In this study, a square packing is assumed for the 224 boreholes – 16 × 14 boreholes with 2.13 m spacing implies a surface area of 31.95 m × 27.69 m. Due to symmetry, only a quarter of the geometry is modelled in OpenGeoSys (cf. Catolico *et al*., 2012; Zhang *et al*., 2016) with 8 × 7 boreholes. The domain size is taken to be 30 m × 30 m with a depth of 72 m. Close to the one-dimensional BHEs on the surrounding formation, the mesh is refined according to the size of the BHE radius to ensure accurate results (Diersch *et al.*, 2011b). On all faces of the geometry including the faces of symmetry, a zero heat-flux boundary condition is imposed (figure 6). For the initial condition, the surface temperature and the geothermal gradient are used:

$$T_0 = 10.17 - 0.03592(z) \tag{3}$$

in which z is in meters measured from the top as zero reference. The initial temperature varies only slightly for the depth of 72 m considered (see figure 6).

A thermal power-controlled simulation with a fixed flow rate is used starting from the storage months (simulation starts from April) followed by the months of extraction (table 2). A load profile (figure 7) incorporating base loads and peak loads (added at the end of each month) has been used as the input for the simulation; half-day time intervals have been adopted for the load profile. For the simulation, a timestep of 21600s has been used. It is noted that a quarter of the load is used for the pipe network of 56 connected boreholes due to the symmetrical set-up considered.

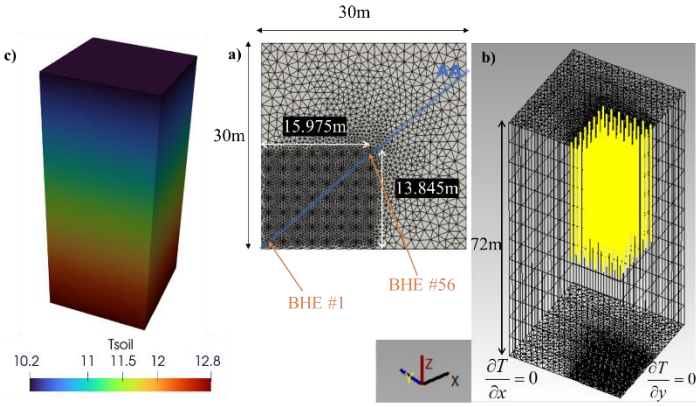


**Figure 6: Finite element mesh for a quarter of the BHE arrays (56 BHEs) showing the top view (a) and side view (b). The initial temperature of the surrounding formation is also shown (c). Line AA cuts through the central (BHE 1) and outermost (BHE 56) BHEs on the diagonal.**

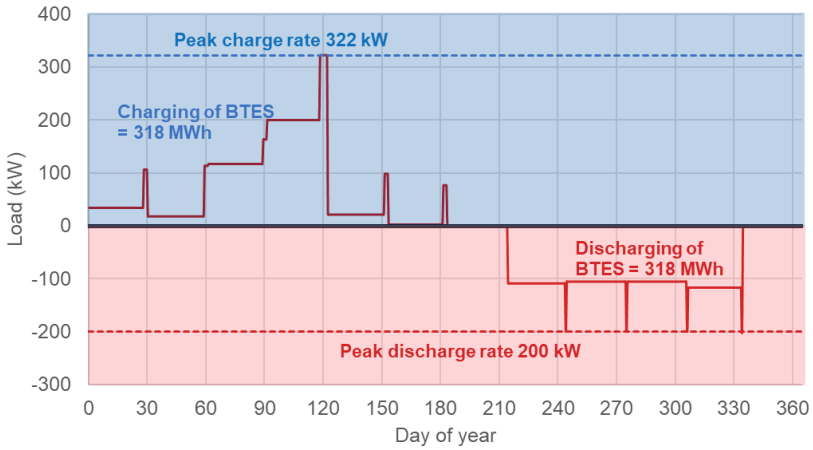


**Figure 7: Applied heat load profile starting from 1st April using half-day time intervals.**

## 4. NUMERICAL RESULTS

The simulation results using the input heat load profile from figure 7 are shown in figure 8. While all BHEs have the same inlet temperature, their outlet temperatures are different (figure 8a). The centred borehole (BHE 1 in figure 6) is expected to have the most extreme (hottest in summer, coldest in winter) outlet temperature and the outermost borehole (BHE 56 in figure 6) is expected to have the lowest outlet temperature during charge. This is because in the central boreholes, there is less heat loss in comparison with the boundary regions which are adjacent to cooler surroundings to which heat is propagated. The plots for these two BHEs are presented in figure 8a. The highest temperature is at 121 days with an inlet temperature of 33.33°C; this corresponds with the month of July which has the highest heat load. At BHE1, the outlet temperature is 30.98°C while at BHE56, it is 30.19°C (Note, that, in this paper, we refer to the outlet temperature $T_{out}$ as the temperature of the fluid leaving the BHE).. At this peak temperature, there is more heat transfer to BHE 56 which has a temperature differential of 3.14°C between the inlet and outlet flow while the temperature differential is 2.35°C for BHE 1. After July, there is a reduction in the amount of heat charged to the ground and the temperatures also reduce. However, it is observed that while BHE 56 is transferring heat to the ground (outlet temperature $T_{out}$ is lower than inlet temperature $T_{in}$), BHE 1 starts losing heat in September as seen from $T_{out} > T_{in}$. This implies that in September, the central part of the array is maximally charged, and it starts to lose heat to the surroundings. On the other hand, the boundary of the array is less efficient at retaining thermal charge. The lowest temperatures in the BTES correspond with the end of the discharge period. The lowest outlet temperatures are 3.80°C and 4.24°C for BHE1 and BHE56 respectively, with an inlet temperature of 2.19°C.

During discharge/extraction, heat is extracted from BHE 1 at a steady rate with an average temperature differential of 1°C. At the boundary however (BHE 56), heat extraction gradually increases to a temperature change of 1.33°C. This can again be attributed to the surrounding colder formation to which heat is transferred. Heat transfer through the boundary is clear from figures 8b and 8c in which the thermal front is shown. During injection, heat is propagating outwards from the hotter boreholes to the cooler surroundings, but during extraction, the conduction is from the hotter surroundings to the cooler boreholes. During the first 'rest' period (October), although no heat load is applied, BHE1 is discharging heat from the ground to the fluid, while BHE56 is still

charging heat from the fluid to the ground, due to the assumed continuous fluid flow (although in reality, at times of no thermal load, fluid circulation would likely cease to save circulation pumping costs and to prevent unwanted redistribution of heat from the centre of the array to the periphery). In the second rest period (March), the opposite applies (Figure 10), and an overall rapid increase in fluid temperature is observed, signifying onset of recovery. Following the peak loads applied at the end of each month (cf. figure 7), corresponding spikes are seen for both charge and discharge periods.

Figure 8d shows the temperature of the ground during peak charge and peak extraction. Temperatures at shallow depth are higher than at the base of the array during the charging cycle. This is likely because of the direction of fluid flow (down the borehole annulus): during charge, hot fluid enters the borehole annulus at the top and progressively loses heat and temperature as it descends. Some authors have suggested that optimal charging can be achieved by reversing fluid flow during charge cycles (i.e., entering borehole annulus at base and flowing upwards – Andersson et al. 2021). In our modelled scenario, during extraction, the fluid is colder at the top as it gains heat as it descends. It is also noted that the thermal front during peak injection (extending to ~27m) is less than the thermal front during peak extraction (extending to ~35m) – Figures 8b,c. This is simply related to elapsed time (and our decision to commence the simulation with a charge cycle); as the simulation progresses thermal effects propagate out into surrounding rock.. Figure 9 shows the temperature distribution within the storage volume (rock) with time. The BHEs gradually transfer heat to the rock during the injection/charge phase and reduction in the rock temperature is shown during the extraction phase. The initial condition (0 day) and final (334 days) temperature conditions are similar, as heat extraction balances heat injection. The change in temperature between the inlet and outlet for BHE 1 and BHE 56 is shown in Figure 10. For BHE 56, heat is being injected to the ground during charge and heat is extracted from the ground during extraction. However, For BHE 1, even though heat is being injected in September, heat losses dominate outside peak rates. In the extraction phase, both BHEs extract heat from the ground.

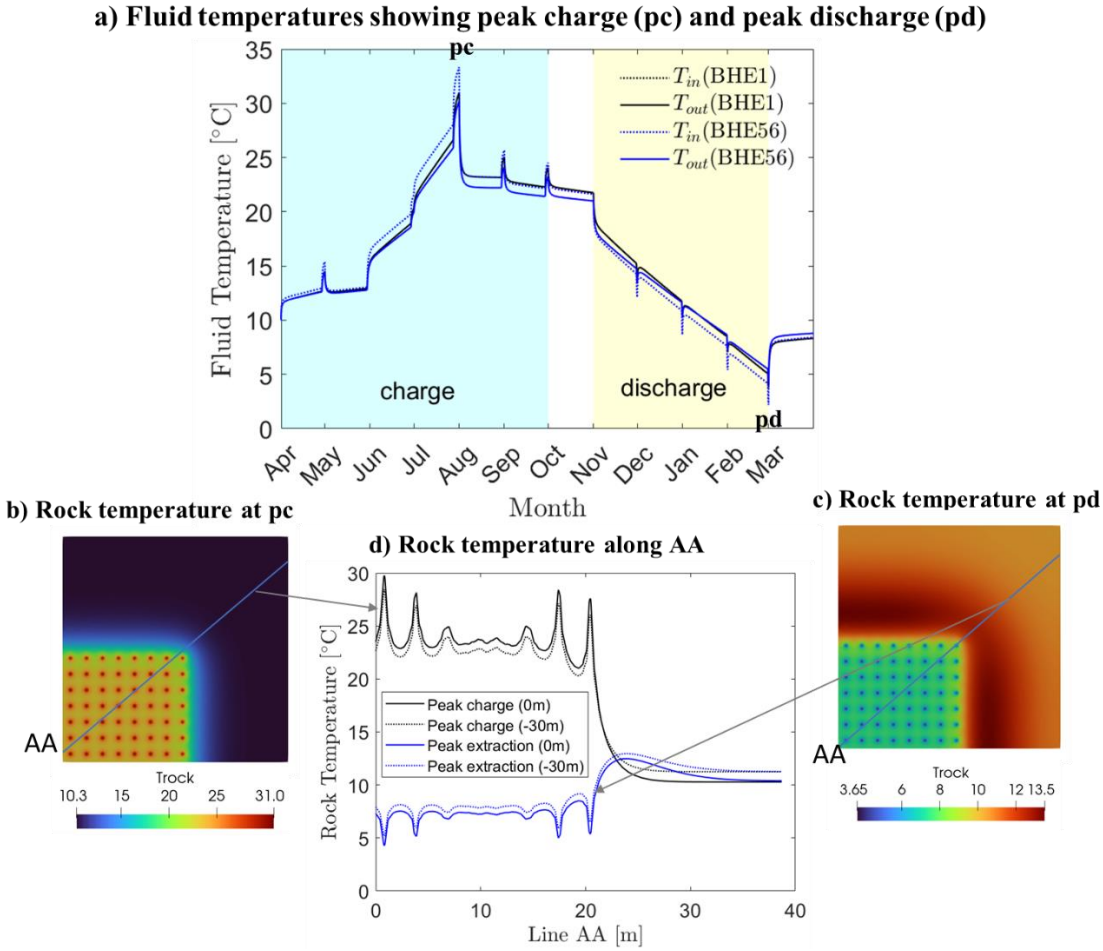


**Figure 8: BHE and rock temperatures with constant heat load: (a) fluid temperatures for inner (BHE1) and outer (BHE56) BHEs; (b) rock temperature at period of highest temperature (peak charge); (c) rock temperature at period of lowest temperature (peak extraction); (d) rock temperature along line AA.**

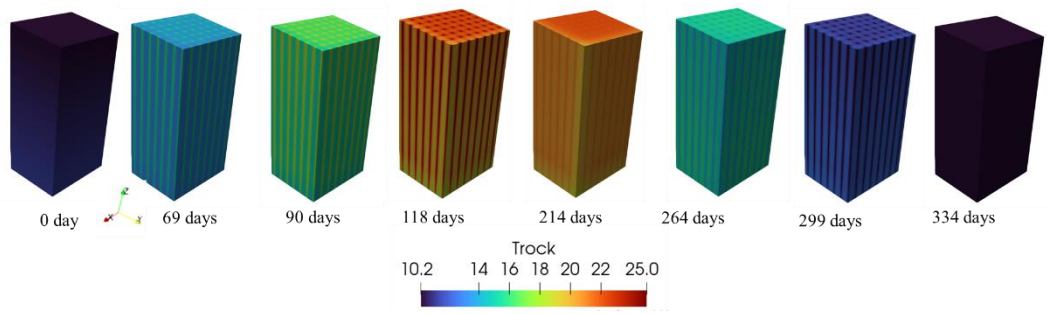


**Figure 9: Temperature distribution of storage volume (15.975×13.845×36 m$^3$) at different times during the year. View is shown from the boundary of the storage volume.**

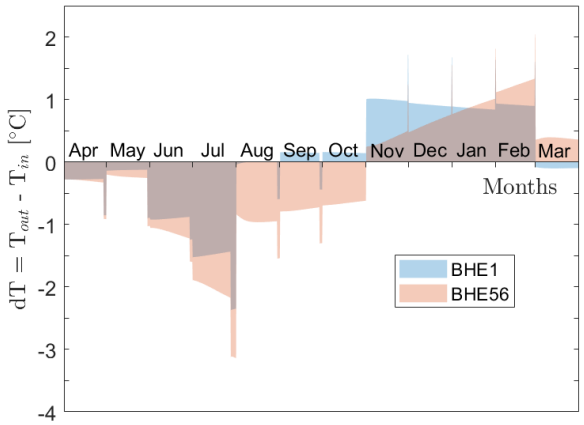


**Figure 10: Change in temperature between the inlet and outlet flow temperatures for BHE 1 and BHE 56.**

## 5. DISCUSSION AND CONCLUSION

The James Watt building in the University of Glasgow has a heat demand of 3011 MWh (11196 GJ) per annum. Solar-thermal analysis performed using Atlite showed that, using solar panels installed on a space 1.5 times the size of the building's roof size, it is possible to meet the building's heat demand in summer months (April – September ≈ 1030 MWh) and store the surplus heat using borehole thermal energy storage. Based on the assumptions in this study, around 318 MWh (1144.8 GJ) surplus summer solar energy was found to be available for storage per annum. The BTES system was charged with this amount of heat over a period of 6 months (April – September). To maintain a balanced subsurface system, the same amount of heat injected was evenly extracted from November to February with no charge/extraction in October and March. The borehole array simulated (based on a preliminary evaluation) comprised 224 boreholes each 36 m long and 2.13 m spacing assuming square packing of boreholes. Further optimisation would almost certainly improve the array design and borehole spacing. A quarter of the borehole geometry was used for simulating the subsurface BTES system assuming rock properties relevant for the Glasgow area.

A simulation driven by the heat loads as input was run for a period of one year. Results showed that the central BHEs achieve a slightly higher outlet temperature compared to the outer boreholes with a recorded maximum fluid outlet temperature of 30.98°C in the central BHE 1 compared to 30.19°C at the outer BHE 56. The minimum fluid inlet temperature in the BHEs was 2.19°C; i.e. above the freezing point of water, but close enough that an anti-freeze solution was used as a heat transfer fluid. This implies that for the first year, the BTES system can provide 318 MWh (1144.8 GJ) out of 1981 MWh (7131.6 GJ) required for the winter months in the James Watt building, representing 16% of the winter heat demand (and arguably more, once the energy contributed by the heat pump compressor is considered). The temperature change between the inlet and outlet flow streams showed that there was more heat transfer at the boundaries of the array (BHE 56) compared to BHE 1. The coupled OpenGeoSys-TESPy platform adopted in this work enabled an investigation of the fluid and rock temperatures and confirmed the possibility of meeting some of the James Watt building heat demand using solar borehole thermal energy storage. In the summer, the complete heat demand of 1030 MWh is met using solar-thermal with a surplus of 318 MWh. This surplus is stored and is used to contribute to the 1981 MWh heat demand of the building in winter. Future work will look at the operation of the system beyond one year and the effects of operational parameters such as flow rate and borehole configuration. The James Watt building also has a space cooling demand, which we have ignored in our simulations as data were not available, but this could also theoretically be used to meet heat demand or used for seasonal storage. While numerical modelling has proven capable of performing these simulations, it is computationally demanding and time consuming. Analytical models (Earth Energy Designer, GLHEPro and others) are available that can perform wholly adequate simulations of this scenario with a fraction of the computer power and processing time. Very preliminary comparisons of our results with those generated by Earth Energy Designer (EED) suggest an overall good correspondence, but that EED results in somewhat more extreme fluid temperatures during peak loads. This discrepancy may be explained by the time step used in our simulations, or by the more nuanced way in which EED calculates borehole thermal resistance from fluid flow rates and turbulence. This comparison will be investigated and published in future research.

**ACKNOWLEDGEMENT**

This work was supported by the UK Engineering and Physical Sciences Research Council (EPSRC) grant EP/T023112/1 for the INTEGRATE (Integrating seasoNal Thermal storagE with multiple enerGy souRces to decArobonise Thermal Energy) project.

**REFERENCES**

Al-Khoury, R., Kölbel, T. and Schramedei, R.: Efficient numerical modeling of borehole heat exchangers. *Computers & Geosciences* 36, no. 10 (2010), 1301-1315.

Andersson, O., Håkansson, N. & Rydell, L. (2021). Heat pumps rescued Xylem's heat storage facility in Emmaboda, Sweden. *REHVA Journal* 54(4), 23-27. https://www.rehva.eu/rehva-journal/chapter/default-cb84adc317-8

Banks, David. *An introduction to thermogeology: Ground source heating and cooling*. John Wiley & Sons, (2012).

BEIS: Digest of UK Energy Statistics (Dukes): Renewable Sources of Energy. DUKES chapter 6: statistics on energy from renewable sources, (2022).

BEIS: Energy consumption in the UK 2021, (2021). https://www.gov.uk/government/statistics/energy-consumption-in-the-uk-2021 (accessed September 14, 2022)

BEIS: Energy white paper: Powering our net zero future, (2020). https://www.gov.uk/government/publications/energy-white-paper-powering-our-net-zero-future (accessed February 26, 2021).

Brown, C. S., Kolo, I., Falcone, G., & Banks, D.: Repurposing a Deep Geothermal Exploration Well for Borehole Thermal Energy Storage: Implications from Statistical Modelling and Sensitivity Analysis. *Applied Thermal Engineering*, 119701, (2022).

Browne, M.A.E., Robins, N.S., Evans, R.B., Monro, S.K. and Robson, P.G. 1987.: *The Upper Devonian and Carboniferous sandstones of the Midland Valley of Scotland. Investigation of the geothermal potential of the UK*. British Geological Survey, HMSO, Keyworth, (1987).

Cai, W., Wang, F., Chen, S., Chen, C., Liu, J., Deng, J., Kolditz, F. and Shao, H.: Analysis of heat extraction performance and long-term sustainability for multiple deep borehole heat exchanger array: A project-based study. *Applied Energy* 289 (2021), 116590.

Catolico, N., Ge, S. and McCartney, J. S.: Numerical modeling of a soil-borehole thermal energy storage system. *Vadose Zone Journal* 15, no. 1 (2016), 1-17.

Chen, C., Shao, H., Naumov, D., Kong, Y., Tu, K. and Kolditz, O.: Numerical investigation on the performance, sustainability, and efficiency of the deep borehole heat exchanger system for building heating. *Geothermal Energy* 7, no. 1 (2019), 1-26.

Diersch, H-JG, Bauer, D., Heidemann, W., Rühaak, W. and Schätzl, P.: Finite element modeling of borehole heat exchanger systems: Part 1. Fundamentals. *Computers & Geosciences* 37, no. 8 (2011), 1122-1135.

Diersch, H-JG, Bauer, D., Heidemann, W., Rühaak, W. and Schätzl, P.: Finite element modeling of borehole heat exchanger systems: Part 2. Numerical simulation. *Computers & Geosciences* 37, no. 8 (2011b), 1136-1147.

EC (European Commission): Renewables steadily increasing in heating and cooling, (2022), https://ec.europa.eu/eurostat/web/products-eurostat-news/-/edn-20220211-1 (accessed September 14, 2022).

Energy Systems Catapult: A Guide to Decarbonisation of Heat. (2022), https://es.catapult.org.uk/guide/decarbonisation-heat/#:~:text=Heating%20accounts%20for%20about%2037,Hot%20water%20%3D%204%25 (accessed September 14, 2022).

Forsyth, I.H., Hall, I.H.S. and McMillan, A.A.: Geology of the Airdrie district. Sheet 31W (Scotland). *Memoir of the British Geological Survey*. British Geological Survey, Keyworth, (1996).

Gao, L., Zhao, J., and Tang, Z.: A review on borehole seasonal solar thermal energy storage." *Energy Procedia* 70 (2015), 209-218.

Gehlin, S. Borehole thermal energy storage. *Advances in ground-source heat pump systems*, 2016, 295-327.

Google Maps. Map of UK showing the James Watt Building, (2022), (accessed September 15, 2022).

Hall, I.H.S., Browne, M.A.E. & Forsyth, I.H.: Geology of the Glasgow district: Memoir for 1: 50 000 Geological Sheet 30E. *Memoir of the British Geological Survey*. British Geological Survey, Keyworth, (1998).

Henning, H-M., and Palzer, A.: A comprehensive model for the German electricity and heat sector in a future energy system with a dominant contribution from renewable energy technologies—Part I: Methodology. *Renewable and Sustainable Energy Reviews* 30 (2014), 1003-1018.

Hersbach, H., Bell, B., Berrisford, P., Hirahara, S., Horányi, A., Muñoz-Sabater, J., Nicolas, J. et al.: The ERA5 global reanalysis. *Quarterly Journal of the Royal Meteorological Society* 146, no. 730 (2020), 1999-2049.

Hofmann, F., Hampp, J., Neumann, F., Brown, T. and Hörsch. J.: Atlite: a lightweight Python package for calculating renewable power potentials and time series. *Journal of Open Source Software* 6, no. 62 (2021), 3294.

Kolo, I., Brown, C. S., Falcone, G. and Banks, D.: Closed-loop Deep Borehole Heat Exchanger: Newcastle Science Central Deep Geothermal Borehole. (2022). In *European Geothermal Congress 2022.*

Kubiński, Kamil, and Szabłowski, Ł.: Dynamic model of solar heating plant with seasonal thermal energy storage. *Renewable Energy* 145 (2020), 2025-2033.

Lyden, A., Brown, C. S., Kolo, I., Falcone, G., and Friedrich, D.: Seasonal thermal energy storage in smart energy systems: District-level applications and modelling approaches, *Renewable and Sustainable Energy Reviews* 167 (2022), 112760.

Maximov, S. A., Mehmood, S. and Friedrich, D.: Multi-objective optimisation of a solar district heating network with seasonal storage for conditions in cities of southern Chile. *Sustainable Cities and Society* 73 (2021), 103087.

Melinder, Å.: *Properties of Secondary Work Fluids for Indirect Systems*. International Institute of Refrigeration, Paris, France, (2010).

Met Office: Historic Station Data: Paisley. [Online], 2022. Available at: https://www.metoffice.gov.uk/pub/data/weather/uk/climate/stationdata/paisleydata.txt (accessed October 2, 2022).

Nordell, B. O., and Hellström, G.: High temperature solar heated seasonal storage system for low temperature heating of buildings. *Solar energy* 69, no. 6 (2000), 511-523.

Pahud, D.: Central solar heating plants with seasonal duct storage and short-term water storage: design guidelines obtained by dynamic system simulations. *Solar Energy* 69, no. 6 (2000), 495-509.

Quaggiotto, D., Zarrella, A., Emmi, G., De Carli, M., Pockelé, L., Vercruysse, J., Psyk, M. et al.: Simulation-based comparison between the thermal behavior of coaxial and double U-tube borehole heat exchangers. *Energies* 12, no. 12 (2019), 2321.

Saloux, E., and Candanedo, J. A.: Model-based predictive control to minimize primary energy use in a solar district heating system with seasonal thermal energy storage. *Applied Energy* 291 (2021), 116840.

Salvestroni, M., Pierucci, G., Pourreza, A., Fagioli, F., Taddei, F., Messeri, M. and De Lucia, M.: Design of a solar district heating system with seasonal storage in Italy. *Applied Thermal Engineering* 197 (2021), 117438.

Schach, R., & Wollstein-Lehmkuhl, A. E.: Decentralized heat supply with seasonal heat storage systems: Comparison of different heating systems. *Energy Procedia*, *155* (2018), 320-328.

Schulte, D. O., Rühaak, W., Oladyshkin, S., Welsch, B. and Sass, I.: Optimization of medium-deep borehole thermal energy storage systems. *Energy Technology* 4, no. 1 (2016), 104-113.

Skarphagen, H., Banks, D., Frengstad, B. S., & Gether, H.: Design considerations for borehole thermal energy storage (BTES): A review with emphasis on convective heat transfer. *Geofluids*, *2019* (2019).

Wang, H. and Qi, C.: Performance study of underground thermal storage in a solar-ground coupled heat pump system for residential buildings. *Energy and Buildings*, 40, (2008), 1278-1286.

Watson, S.M., Westaway, R & Burnside, N.M.: Digging deeper: The influence of historical mining on Glasgow's subsurface thermal state to inform geothermal research. *Scottish Journal of Geology* 55 (2019), 107-123. doi: 10.1144/sjg2019-012

Watson, S. M.: An investigation of the geothermal potential of the Upper Devonian sandstones beneath eastern Glasgow. PhD diss., University of Glasgow, 2022.

Wood, C. J., Hao L. and Riffat, S. B.: Comparative performance of 'U-tube' and 'coaxial' loop designs for use with a ground source heat pump. *Applied Thermal Engineering* 37 (2012), 190-195.

Xu, J., Wang, R. Z., and Li, Y.: A review of available technologies for seasonal thermal energy storage. *Solar energy* 103 (2014), 610-638.

Xu, J., Li, Y., Wang, R. Z. and Liu, W.: Performance investigation of a solar heating system with underground seasonal energy storage for greenhouse application. *Energy* 67 (2014b), 63-73.

Yuan, X., Heikari, L., Hirvonen, J., Liang, Y., Virtanen, M., Kosonen, R., and Pan, Y.: System modelling and optimization of a low temperature local hybrid energy system based on solar energy for a residential district. *Energy Conversion and Management* 267 (2022), 115918.

Zhang, R., Lu, N. and Wu, Y.: Efficiency of a community-scale borehole thermal energy storage technique for solar thermal energy. In *GeoCongress 2012: State of the Art and Practice in Geotechnical Engineering*, (2012), pp. 4386-4395.